An Enhanced Thermoelectric Collaborative Cooling System with Thermoelectric Generator Serving as a Supplementary Power Source

Ning Wang, *Member, IEEE,* Jian-Nan Zhang, Zhi-Yuan Liu, Can Ding, *Member, IEEE,* Guo-Rong Sui, *Senior Member, IEEE,* Hong-Zhi Jia and Xiu-Min Gao

***Abstract*— Thermoelectric coolers (TECs) are widely used in state-of-the-art thermal management systems. Recently, there is a big trend that is to power TECs using thermoelectric generators (TEGs). Mainstream research efforts focus on attaining a higher figure of merit (*ZT*) of thermoelectric material, which now faces a great challenge. Alternatively, this paper proposes a different approach to improve the performance of TEC, i.e., integration of a thermoelectric generator (TEG) with a TEC. The TEG converts the collected heat energy into electric current, which reduces the power consumption and enhances the cooling capacity of the TEC. Using different methods of connecting the TEC and TEG, two thermoelectric collaborative cooling systems are proposed. Accurate SPICE models of the two cooling systems are established. Experimental results demonstrate that the discrepancy between the currents flowing through the TEC in the experiments and in the SPICE models is less than 4.8% on average. Based on the verified SPICE models, the proposed TEC-TEG collaborative cooling systems are assessed in terms of power consumption, cooling capacity, coefficient of performance, and cooling efficiency. Compared with a typical Peltier cooling system, the two collaborative cooling systems achieve significant performance improvements.**

***Index Terms*— Energy harvesting, collaborative cooling, electro-thermal conversion, thermoelectric cooler (TEC), thermoelectric generator (TEG).**

I. Introduction

THE rapidly growing integrated circuits (ICs) industry has pushed engineers to place a dramatically increasing number of transistors into an IC chip with continuously shrinking size. Massive transistors opening and closing at a high frequency result in tremendous power consumption, which leads to a significant temperature increase in the chips. Although a recent research has shown that high temperature compensated voltage reference integrated circuit [1] fabricated by silicon carbide (SiC) material is able to work at up to 300℃, such high temperatures inevitably have many negative effects. For example, temperature rises can cause gate leakage current [2] and introduce threshold voltage variation in MOS transistors [3]. Moreover, the temperature difference between various parts of the clock tree can exacerbate clock skew [4].

Developing an effective measure for cooling ICs is a crucial, but challenging, task. Many works have been done to address this issue, including air-cooling [5], water-cooling [6], and air-water hybrid cooling [7]. However, it is difficult to integrate these traditional methods with IC systems. Thermoelectric cooler (TEC) is a solid-state device which is able to transfer heat from one side of the device to the other with the consumption of electrical energy. It is the most suitable and promising cooling solution for IC systems and has attracted considerable attention [8-11] due to its small size and ease of integration in IC chips.

TEC is implemented using thermoelectric material. To evaluate properties of thermoelectric materials, the most important performance index is the dimensionless figure of merit *ZT* that measures the electro-thermal conversion efficiency. *ZT* is defined as

$$ZT = \frac{S^2 \sigma T}{\kappa} \tag{1}$$

where S is Seebeck coefficient, σ is electrical conductivity, κ is thermal conductivity, and T is temperature. To improve the performance of TEC, many works [12-14] attempted to maximize the coefficient of performance (COP) or cooling capacity (Q_c) of TEC by applying external current/voltage sources and determining the best working conditions. Another approach is to use a thermoelectric generator (TEG) [15-21] as an energy harvesting engine for TEC, leading to self-powered TEC-TEG combined cooling systems [22-28]. For example, in [22], the possibility of using solar TEG to power TEC was investigated. The results show that ten solar TEG modules are required to power a small TEC at optimum performance. Manikandan and Kaushik studied a TEC-TEG combined system using the maximum power point tracking (MPPT) technique to maximize the cooling power and overall efficiency [25]. With the MPPT technique, the overall efficiency can be increased from 2.606% to 4.375% when the temperature difference between the two sides of the TEG is 150 K and that of the TEC is 10 K. A TEG-TEC integrated system was proposed with two separated single-stage TEGs [27]. With the multi-objective optimization, the maximum cooling capacity was improved by 35.33%. Also, Wiriyasart [28] presented a thermoelectric closed-loop control method based on TEC and TEG systems. By increasing the number of TEGs, the thermal performance of the TEC system was enhanced, further resulting in a greater temperature difference for TEGs system. The available TEC-TEG combined cooling systems use TEG as the only power source for TEC. However, due to the low thermo-

Manuscript received; This work was supported in part by NSFC under Grant 61804096, in part by the National Key Research and Development Plan--Earth Observation and Navigation Key Special Project under Grant 2017YFB0503102, in part by the National Key Research and Development Program of China under Grant 2018YFC1313803 and 2018YFA0701800. (Corresponding author: Can Ding)

N. Wang, J.-N. Zhang, Z.-Y. Liu, G.-R. Sui, H.-Z. Jia and X.-M. Gao are with the Engineering Research Center of Optical Instrument and System, Ministry of Education, Shanghai Key Laboratory of Modern Optical System, University of Shanghai for Science and Technology, Shanghai 200093, China (e-mail: nwang@usst.edu.cn).

C. Ding is with the Global Big Data Technologies Center, University of Technology Sydney, Sydney, NSW 2007, Australia (e-mail: can.ding.1989@gmail.com).

electric conversion efficiency of currently TEGs, most existing TEC-TEG combined cooling systems require multiple TEGs to power TEC and the cooling performance is limited.

In this paper, we propose to use TEG as a supplementary power source for TEC to save the power supply from main source and to improve cooling performance. Unlike previous configurations in which where TECs and TEGs are connected in series, this paper reports two different methods to incorporate TEG with TEC. SPICE models of the two systems are established, optimized, and verified by experiment. The results show that the proposed two systems significantly improve the performance compared to the typical cooling model.

The rest of the paper is organized as follows. Following the introduction, typical cooling model and key parameters of TEC are reviewed in Section II. In Section III, the schematics and equivalent SPICE models of two different collaborative cooling systems are proposed and verified. Section IV evaluates the performance of the proposed models by SPICE simulation and experiment. Finally, conclusions are drawn in section V.

II. Typical Peltier Cooling Model

A. General Analytical Models of TEC and TEG

TECs and TEGs, are Thermoelectric modules, which are thus correlated with three thermoelectric phenomena involving Seebeck, Peltier, and Thomson effects. The Seebeck effect is the phenomenon whereby the temperature difference between the two sides of a TEG can generate a voltage, which can be calculated by:

$$V_g = S_g \Delta T_g \tag{2}$$

where V_g, S_g and ΔT_g are the Seebeck voltage, Seebeck coefficient, and temperature difference between the two sides of the TEG, respectively. The Peltier effect describes the phenomenon whereby the electric current applied to a TEC can lead to the generation of temperature difference. The heat absorbed at the cold side and released at the hot side is determined by (3) and (4), respectively.

$$Q_c = S_c I_c T_c - \frac{1}{2} I_c^2 R_c - K(T_h - T_c) \tag{3}$$

$$Q_h = S_c I_c T_h + \frac{1}{2} I_c^2 R_c - K(T_h - T_c) \tag{4}$$

where Q_c, Q_h, T_c, T_h, S_c, I_c, R_c, and K are the heat absorbed at the cold side, heat released at the hot side, temperature at the cold and hot sides, Seebeck coefficient, electric current flowing through the TEC, resistance, and thermal conductivity of the TEC module, respectively. Considering the power generated from working against the Seebeck voltage and Joule power, the electrical power consumption P_e is given by

$$P_e = I_c^2 R_c + S_c I_c (T_h - T_c) \tag{5}$$

Currently, the COP is widely used to describe the cooling performance [12-14]. This can be expressed as

$$\mathrm{COP} = \frac{Q_c}{P_e} = \frac{\left[S_c I_c T_c - \frac{1}{2} I_c^2 R_c - K(T_h - T_c) \right]}{I_c^2 R_c + S_c I_c (T_h - T_c)} \tag{6}$$

However, a more accurate parameter for evaluating the cooling performance is ψ, which comes from exergy analysis, and is given by

$$\psi = \frac{exergy\_out}{exergy\_in} \tag{7}$$

Equation (7) is derived from exergy analysis [29], which defines ψ as the ratio of exergy output and exergy input, where the former is only a part of Q_c and the latter is the electrical power consumption P_e

$$exergy\_in = P_e \tag{8}$$

$$exergy\_out = Q_c \left(\frac{T_h}{T_c} - 1 \right) \tag{9}$$

Thus, ψ can be described as

$$\psi = \frac{Q_c}{P_e} \left(\frac{T_h}{T_c} - 1 \right) \tag{10}$$

Substituting (3) and (5) into (10), ψ can be written as

$$\psi = \frac{\left[S_c I_c T_c - \frac{1}{2} I_c^2 R_c - K(T_h - T_c) \right] \left(\frac{T_h}{T_c} - 1 \right)}{I_c^2 R_c + S_c I_c (T_h - T_c)} \tag{11}$$

The maximum value of ψ is

$$\psi_{\max} = \frac{\sqrt{1 + ZT_m} - \frac{T_h}{T_c}}{1 + \sqrt{1 + ZT_m}} \tag{12}$$

where Z and T_m are defined as

$$Z = \frac{S_c^2}{R_c K} \tag{13}$$

$$T_m = \frac{T_h + T_c}{2} \tag{14}$$

The parameter ψ and the COP will be used to evaluate the performance of the TEC-TEG collaboration systems described in Section III.

B. Typical SPICE Models of TEC and TEG

For the convenience of analyzing the performance of TEC and TEG in electronic circuit terms, the analytical models should be transferred into the equivalent SPICE models by employing the analogies between thermal and electrical variables [30]. Corresponding SPICE models include electrical

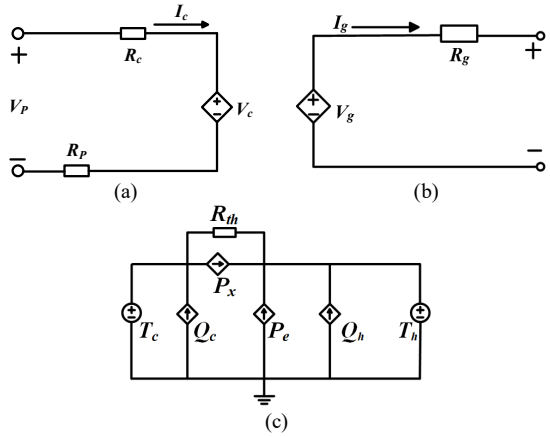

Fig. 1. Equivalent SPICE model of TEC and TEG including: (a) Electrical part of TEC; (b) Electrical part of TEG; (c) Thermal part of TEC and TEG.

TABLE I
SYSTEM SPECIFICATIONS OF THE THERMOELECTRIC MODULES USED IN THIS WORK

Module Name	TEG-450-0.8-1.0	TEC-12710
Dimensions (mm)	54 × 54	40 × 40
I_{max} (A)	0.75	10
ΔT_{max} (°C)	270	66
V_{max} (V)	21	15
P_{max} (W)	5	85
S (V/K)	0.191	0.055
K (W/K)	1.45	0.87
R (Ω)	28	1.8

and thermal parts. The thermal part is usually fixed, while the electrical part, which depends on external circuit structures of the TEC, is changeable. Fig. 1 shows a typical SPICE model of a TEC and a TEG. In the electrical part shown in Fig. 1(a), V_P is a voltage source that drives the TEC to work, R_P is the internal resistance of voltage source, R_c is the internal resistance of the TEC, and V_c is the Seebeck voltage of the TEC. Fig. 1(b) shows the electrical part of the TEG, where R_g and V_g represent the internal resistance and generated voltage of TEG, respectively. In the thermal part as shown in Fig. 1(c), the heat flow Q_c is divided into two parts. One is represented by current source P_x

$$P_x = S_c I_c T_c - \frac{1}{2} I_c^2 R_c \tag{15}$$

where I_c can be formulated according to Fig. 1(a) as

$$I_c = \frac{V_P - S_c \Delta T_c}{R_P + R_c} \tag{16}$$

The second part is the current flowing across the resistance R_{th}, where

$$R_{th} = 1/K \tag{17}$$

The TEG functions as a power supplier and works without a voltage supply. The generated voltage of the TEG depends on the Seebeck coefficient and the temperature difference between the hot and cold sides. Therefore, comparing with TEC, TEG can be modeled as a voltage-controlled voltage source as shown in Fig. 1(b) and Fig. 1(c) with same thermal part but different electrical parts [31].

C. Simulation Setup, Results, and Analysis

Table I lists the basic parameters of the TEC and TEG used in this study. K is the thermal conductance, S is the Seebeck coefficient, and R is the internal resistance of the TEC or TEG. The internal resistance of the voltage source is modeled as an equivalent resistance R_P with a constant approximate value of 2 Ω.

From Eqs. 3 and 5, P_e gradually increases with the increase of V_P while Q_c first increases and then decreases under different working conditions (T_c). In this work, simulations were carried out with fixed hot side temperature T_h=300K [32]. By substituting the values of Q_c and P_e into Eq. 10, the conversion efficiency ψ was obtained. Under different T_c, a peak value of ψ can always be produced by selecting an optimal V_P. The value of ψ can change significantly with different V_P. In this work, we propose to enhance the cooling efficiency of the TEC by connecting it with a TEG to adjust Q_c and P_e. The performance can be improved over a wider range of V_P than a typical Peltier cooling system. However, one could also develop an MPPT technique to make the proposed TEC-TEG collaborative cooling system work at the maximum efficiency by adjusting V_P.

III. SPICE MODELS OF COLLABORATIVE COOLING SYSTEMS

In this work, the heat energy harvested by the TEG is employed as an extra power source for the TEC. By integrating an additional TEG, the performance of the typical Peltier cooling system, which employs only one TEC, can be enhanced. However, note that the way in which TEG is connected with the TEC is of great importance. In this section, two collaborative cooling systems with different connection methods are proposed. The SPICE models of the two systems are developed and then validated through a series of experiments.

A. TEC-TEG Parallel-Connected Cooling (PCC) System

Fig. 2(a) shows the schematic of the proposed TEC-TEG parallel-connected cooling (PCC) system. In this system, the employed TEG has its hot and cold sides connected with a heat source and a heat sink, respectively, which ensures a sufficient temperature difference for the TEG. Through the Seebeck effect, the current generated by the TEG flows across the TEC, contributing to a portion of the power supply.

The thermal part of the system is the same as Fig. 1(c) as the modification is to the external circuit structure rather than the internal topology of the TEC. The electrical part of the SPICE model of the PCC system is shown in Fig. 2(b).

Note that the current flow across the TEC (I_c) is one of the most important parameters in evaluating the cooling performance. By substituting I_c into (3), (6), and (11), the cooling capacity Q_c, power consumption P_e, and overall cooling efficiency ψ of the TEC in this collaborative cooling system can be determined.

According to Kirchhoff's current law, the current flow across the TEC (I_c) in the PCC system can be formulated as

$$I_c = I_g + I_P \tag{18}$$

where I_g and I_p are given by

$$I_P = \frac{V_P - S_c \Delta T_c - I_c R_c}{R_P} \tag{19}$$

$$I_g = \frac{S_g \Delta T_g - I_c R_c - S_c \Delta T_c}{R_g} \tag{20}$$

Substituting (19) and (20) into (18), the expression of I_c can be rewritten as

$$I_c = \left(\frac{V_P - S_c \Delta T_c}{R_P} + \frac{S_g \Delta T_g - S_c \Delta T_c}{R_g}\right) \frac{R_g \parallel R_P \parallel R_c}{R_c} \tag{21}$$

The difference between the currents through the TEC of the proposed PCC system and that of the typical cooling system is

$$\Delta I_{c\_pcc} = \left(\frac{V_P - S_c \Delta T_c}{R_P} + \frac{S_g \Delta T_g - S_c \Delta T_c}{R_g} \right) \frac{1}{\frac{R_c}{R_g} + \frac{R_c}{R_P} + 1} - \frac{V_P - S_c \Delta T_c}{R_P + R_c} \quad (22)$$

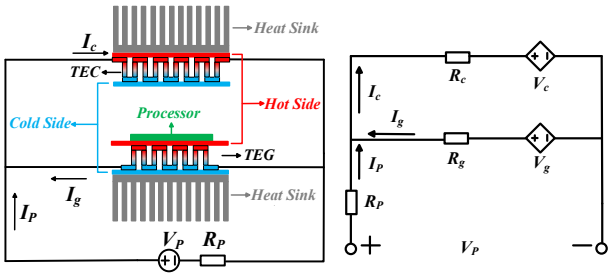

(a) (b)

Fig. 2. (a) Schematic view and (b) electrical SPICE model of the proposed TEC-TEG parallel-connected collaborative (PCC) cooling system.

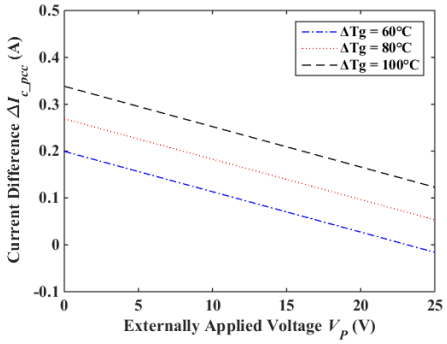

Fig. 3. Calculated difference between the currents through TEC of the proposed PCC system and that of the typical cooling system with different ΔT_g and V_P.

The calculated ΔI_{c_pcc} is plotted in Fig. 3 for different values of ΔT_g and V_P. For most conditions, I_c is larger in the PCC system than in the typical cooling system, indicating an improved cooling performance. However, as the external voltage V_P increases, ΔI_{c_pcc} becomes smaller, indicating that the merit of integrating TEG in the PCC system is decreasing. To avoid this, another method of utilizing the TEG is proposed in the next subsection.

B. Voltage-Controlled Current-Source Cooling (VCC) System

Figs. 4(a) and 4(b) show a schematic view of the proposed voltage-controlled current-source cooling (VCC) system and its electrical part in the equivalent SPICE model. In this system, an operational amplifier (AD741CN) with the specifications listed in Table II is employed. Theoretically, the amplifier has high input resistance with an equal voltage between the in-phase and out-phase ends, which means that no electric current can flow through the out-phase end while V_G generated from the TEG can be exerted on the resistance R_T, which is about 3 Ω calculated by matching the internal resistance of TEC and power supply to obtain large current flowing through TEC. However, in reality, a resistance of 500 KΩ is connected to the input terminal of the AD741CN to minimize the current flow across the TEG.

Assuming the current flow across the TEG is zero, I_g can be written as

$$I_g = \frac{V_g}{R_T} \quad (23)$$

As the current I_c through the TEC in the VCC system is the sum of I_g and I_P, where

$$I_P = \frac{V_P - S_c \Delta T_c - I_c R_c}{R_P} \quad (24)$$

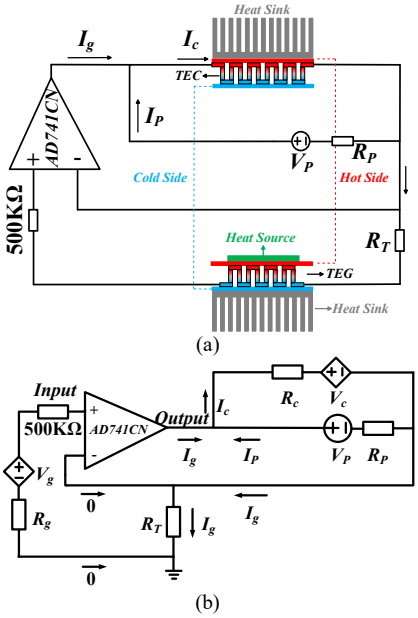

(a) (b)

Fig. 4. (a) Schematic view and (b) electrical SPICE model of the proposed TEC-TEG voltage-controlled current source cooling (VCC) system.

TABLE II
PERFORMANCE SPECIFICATIONS OF AD741CN

Module Name	AD741CN
Supply Voltage (V)	±18
Power Dissipation (mW)	500
Differential Input Voltage (V)	±30
Input Voltage (V)	±15
Quiescent Current (mA)	1.7
Storage Temperature Range (°C)	-65 to +150
Output Short Circuit Duration	Indefinite

I_c can be obtained as follows:

$$I_c = \frac{1}{R_P + R_c} \left[V_P + \frac{V_g R_P}{R_T} - S_c (T_h - T_c) \right] \quad (25)$$

Subsequently, the electric current difference between the VCC system and the typical cooling system can be determined by

$$\Delta I_{c\_vcc} = \frac{V_g R_P}{(R_c + R_P) R_T} = \frac{R_P}{(R_c + R_P)} I_g \quad (26)$$

The calculated ΔI_{c_vcc} is plotted in Fig. 5 for different values of ΔT_g and V_P. It can be concluded from (26) and Fig. 5 that ΔI_{c_vcc} is a positive constant. This means that the proposed VCC system always has a larger current through the TEC than in the typical cooling model. The increment is independent of the externally applied voltage V_P and the internal resistance R_g of the TEG. It should be noted that an extra differential DC source (±18 V) is needed to drive the AD741CN. However, the maximum power consumption of AD741CN is small, i.e., only 550mW. Moreover, when V_p =18 V, the power consumption of

the entire VCC system is 34.74 W, which is significantly larger than that of the amplifier. Thus, the power consumption of the amplifier was neglected in the subsequent calculation.

C. Validation of SPICE Models

The effects of the integrated TEG on the cooling performance for the two models can be evaluated by several parameters such as I_c, Q_c, ΔT_c, and ψ. Among these parameters, only I_c and ΔT_c can be directly obtained from experiments, thus they are used to verify the accuracy of the proposed SPICE models. A specific model in SPICE was used to model AD741CN.

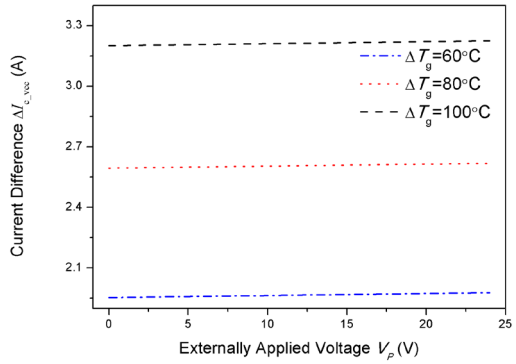

Fig. 5. Calculated difference between the currents through TEC of the proposed VCC system and that of the typical cooling system with different ΔT_g and V_p.

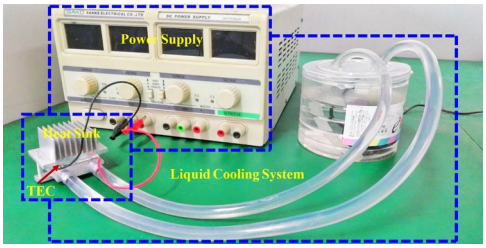

(a)

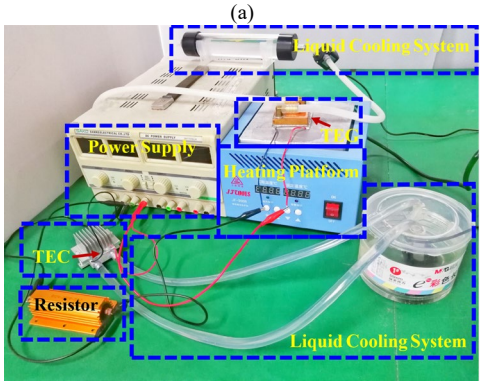

(b)

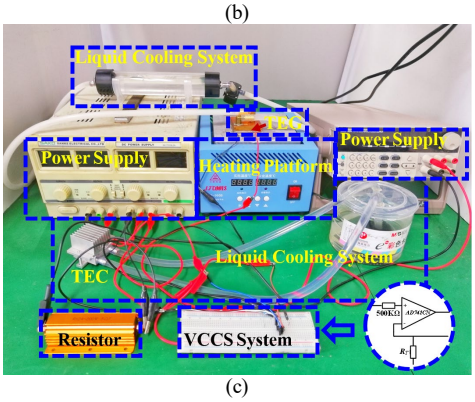

(c)

Fig. 6. Experiment setup of the (a) typical, (b) PCC, and (c) VCC cooling systems.

Figs. 6(a) to 6(c) show the experimental setups for the typical, PCC, and VCC cooling systems, respectively. The temperature difference ΔT_c and the current flow I_c across the TEC can be easily measured using a thermometer and multimeter. Note that the thermometer and multimeter are not shown in Fig. 6 for reasons of clarity. As shown in Fig. 6, water tanks were used to stabilize the cold side temperature of TEC and TEG in experiments. The water tanks had a capacity of about 500 ml and the maximum value of Q_c was up to 37.3 W, which is sufficient for experiments lasting several minutes. Additionally, a high-power resistor was used in the experimental setup to represent the R_P of 2 Ω, this was used to regulate the current flow across TEC in this work. We used a high-power resistor because the current flow across it can be as large as 2 A while a low-power resistor could be damaged by the large current.

Figs. 7(a) to 7(c) plot the simulated and measured variations of I_c with V_P in the typical Peltier, PCC, and VCC systems, respectively, with the temperature difference ΔT_c fixed at 60℃.

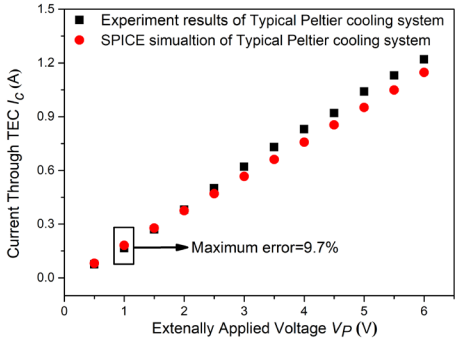

(a)

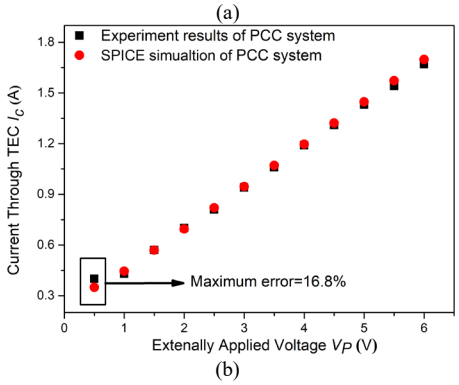

(b)

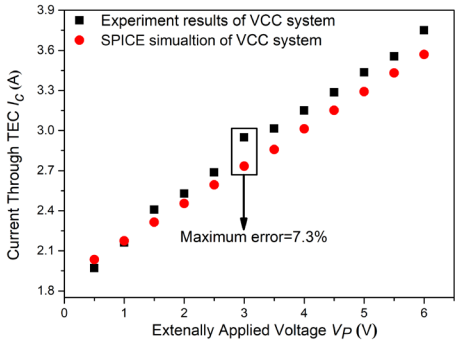

(c)

Fig. 7. Simulated and measured variation of I_c with V_p of the (a) typical Peltier, (b) PCC, and (c) VCC systems with ΔT_c = 60^{0}C.

TABLE III
RELATIVE ERROR OF PROPOSED SPICE MODEL FOR THE PCC AND VCC SYSTEMS UNDER DIFFERENT ΔT_C

Temperature difference of TEG (°C)	Average relative error (%)		Maximum relative error (%)	
	PCC	VCC	PCC	VCC
60	3.6	4.0	16.8	7.3
80	4.7	5.8	12.5	10.5
100	2.3	5.1	12.2	13.7

It is observed from the figures that the simulated I_c agree quite well with the measured results. Compared with typical Peltier and PCC systems, a higher current value can be obtained using PCC system at the same externally applied voltage. Moreover, Table III summarizes the average and maximum relative errors of the proposed collaborative systems under different ΔT_c.

The limited experimental conditions in our laboratory, means that the test results are not very precise. To overcome this limitation, each system was tested five times and the average value was used. As the typical, PCC, and VCC cooling systems were tested in a similar environment, we can conclude that the results showing that PCC and VCC systems outperform the typical Peltier cooling system, despite some possible test errors. This is a promising result.

IV. RESULTS AND DISCUSSION

As the SPICE models were verified by comparing the current through the TEC in the experimental and SPICE simulations, the current-dependent parameters obtained from the SPICE simulation can be considered accurate and used to evaluate the cooling performance. These parameters include the power consumption ratio RP_e, cooling capacity Q_c, COP, and electro-thermal conversion efficiency ψ.

Note that Q_c, COP, and ψ can be obtained by substituting I_c into (3), (6), and (10), respectively. The power consumption ratio RP_e is defined as the ratio of the power supply from the heat source (TEG) and the power supply from the voltage source:

$$RP_e = \frac{P_{e\_hs}}{P_{e\_vs}} \tag{27}$$

For the typical Peltier cooling system which only has a TEC, the external voltage source is the only power supply, and so RP_e=0. For the PCC system, according to Fig. 2(b),

$$P_{e\_hs} = V_g I_g - I_g^2 R_g \tag{28}$$

$$P_{e\_vs} = V_P I_P - I_P^2 R_P \tag{29}$$

Therefore, RP_e for the PCC system can be obtained by substituting (28) and (29) into (27). Different from the PCC system, the power supply from the heat source (P_{e_hs}) of the VCC system cannot be simply determined from (28) because the circuit structure has been changed. Alternatively, P_{e_hs} can be obtained using the total power consumption of the TEC minus the power supply from the voltage source:

$$P_{e\_hs} = P_e - P_{e\_vs} \tag{30}$$

By substituting (30) and (4) into (27), RP_e can be determined for the VCC system. The calculated values of RP_e, Q_c, COP, and ψ in the typical Peltier, PCC, and VCC systems under condition of T_H =300K, ΔT_g = 80°C, and V_P ranging from 4 V to 30 V when the cold side temperature of the TEC is specified at 263K, 273K, and 283K are summarized in Tables IV and V.

As illustrated in Table IV, the power consumption ratio RP_e has a maximum (average) value of 3.67/1 (0.42/1) for the PCC system and 11.03/1 (1.07/1) for the VCC system. This indicates that the heat energy harvested by the TEG constitutes a significant portion of the total power supply in the proposed collaborative systems. Moreover, compared with the typical cooling system, the increment of the maximum (average) cooling capacity in various operating voltages can exceed 3% (18%) for the PCC system, and a further enhancement 9% (33%) can be observed for the VCC system.

Also, as shown in Table V, the two collaborative cooling systems have significantly improved performance compared to the typical Peltier cooling system in terms of the coefficient of

TABLE IV
COMPARISON IN TERMS OF RP_E AND Q_C BETWEEN THE TYPICAL COOLING SYSTEM AND THE PROPOSED COLLABORATIVE COOLING SYSTEMS UNDER CONDITION OF T_H=300K, ΔT_G=80°C, AND V_P RANGES FROM 4V TO 30V WHEN T_C= 263K, 273K, AND 283K.

Parameters		**Power consumption ratio RP_e**			**Cooling capacity Q_c (W)**				
Temp. (K)	Value	Systems			Systems			Comparison	
		Typical	**PCC**	**VCC**	**Typical**	**PCC**	**VCC**	**(PCC-Typical)/Typical**	**(VCC-Typical)/Typical**
263	Max.	0/1	0.85/1	4.69/1	20.04	20.81	22.63	3.85%	12.94%
	Ave.	0/1	0.2/1	0.77/1	14.19	17.22	20.87	21.35%	47.07%
273	Max.	0/1	3.67/1	11.03/1	27.01	27.91	29.90	3.32%	10.71%
	Ave.	0/1	0.42/1	1.07/1	19.12	22.76	26.44	19.04%	38.29%
283	Max.	0/1	3.02/1	7.09/1	34.06	35.09	37.27	3.05%	9.41%
	Ave.	0/1	0.37/1	0.88/1	23.81	28.18	31.89	18.36%	33.92%

TABLE V
COMPARISON IN TERMS OF COP AND Ψ BETWEEN THE TYPICAL COOLING SYSTEM AND THE PROPOSED COLLABORATIVE COOLING SYSTEMS UNDER CONDITION OF T_H=300K, ΔT_G=80°C, AND V_P RANGES FROM 4V TO 30V WHEN T_C= 263K, 273K, AND 283K.

Parameters		**COP**					**ψ (%)**				
Temp. (K)	Value	Systems			Comparison		Systems			Comparison	
		Typical	**PCC**	**VCC**	**PCC/Typical**	**VCC/Typical**	**Typical**	**PCC**	**VCC**	**PCC/Typical**	**VCC/Typical**
263	Max.	0.49	0.77	1.88	1.57	3.84	6.91	9.07	15.63	1.31	2.26

	Ave.	0.35	0.47	0.75	1.34	2.14	4.97	6.33	8.03	1.28	1.62
273	Max.	0.90	2.22	4.58	2.47	5.09	8.91	18.2	88.53	2.04	9.93
	Ave.	0.59	0.86	1.28	1.46	2.17	5.87	8.57	13.01	1.46	2.22
283	Max.	1.80	8.13	18.2	4.52	10.1	10.8	43.4	84.8	4.02	7.86
	Ave.	0.97	1.70	2.75	1.75	2.84	5.81	8.96	11.67	1.54	2.01

TABLE VI
PERFORMANCE SPECIFICATIONS OF THE PROPOSED PCC AND VCC COOLING SYSTEMS

Cooling Systems	PCC	VCC
$Q_{c\ max}$ **(W)**	35.09	37.27
I_{max} **(A)**	1.67	3.75
Ψ_{ave}	0.0896	0.1167
COP$_{ave}$	1.75	2.84

TABLE VII
PERFORMANCE SPECIFICATIONS COMPARISON BETWEEN THE STATE-OF-THE-ART TEC-BASED COOLING SYSTEMS AND THE PROPOSED VCC COOLING SYSTEM

Works	[12]	[13]	[14]	**This Work**
Optimization Mode	Multi-Start Adaptive Random Search	Effectiveness-Number of Transfer Units	Multi-Couple Thermoelectric Cooling	**VCC**
T_c **(K)**	297	275	273	**273**
T_h **(K)**	330	300	300	**300**
P_e **(W)**	14.3	12.72	28.69	**10.11**
Q_c **(W)**	13.33	13.33	13.33	**13.33**
COP	0.932	1.053	0.465	**1.339**
ψ	0.099	0.148	0.065	**0.188**

performance COP and the thermoelectric conversion efficiency ψ. Table VI further summarizes the performance specifications of the proposed PCC and VCC cooling systems. Both of the proposed systems offer improved performance compared with the typical Peltier cooling system. The increment in the VCC system is 2-3× that in the PCC system, which means that the VCC system is applicable in condition where more cooling capacity is required. However, the compactness and ease to integration of the PCC system, make it a more appropriate choice when space is a major constraint.

Moreover, to further demonstrate the superiority of the proposed collaborative system, the proposed VCC cooling system is further compared with other state-of-the-art TEC-based cooling systems [12-14] in Table VII. Note that the cooling capacity is determined by the TEC module and the input power. To facilitate a fair comparison, we set all the systems to have the same cooling capacity of Q_c = 13.33 W and compare their power consumption, COP, and overall cooling efficiency. To reach the same cooling capacity, the proposed VCC method has the minimum power consumption. The VCC method also obtains the maximum COP of 1.339 and the maximum conversion efficiency ψ of up to 0.188.

V. CONCLUSION

This paper, has described two TEC-TEG collaborative cooling systems, namely the parallel-connected cooling (PCC) system and the voltage-controlled current-source cooling (VCC) system. These systems provide an alternative approach to improve the performance of TEC-based cooling systems. SPICE models of the two collaborative systems were developed and verified through a series of experiments. By comparing the currents flowing across the TEC in the simulations and experiments, the accuracy of the developed SPICE models was validated. Subsequently, the power consumption ratio RP_e, cooling capacity Q_c, COP, and electro-thermal conversion efficiency ψ of the two collaborative cooling systems were obtained via SPICE simulations. They were then compared with those of the typical Peltier cooling system to demonstrate the superiority of the PCC and VCC systems.

REFERENCES

[1] V. Banu, P. Godiggnon, M. Alexandru, M. Vellveh, X. Jordà, and J. Millán, "High Temperature-Low Temperature Coefficient Analog Voltage Reference Integrated Circuit Implemented with SiC MESFETs," in *European Solid-State Circuits Conf.*, 2013, pp. 427-430, doi: 10.1109/ESSCIRC.2013.6649164.

[2] S. Turuvekere, D. S. Rawal, A. Dasgupta, and N. Dasgupta, "Evidence of Fowler-Nordheim tunneling in gate leakage current of AlGaN/GaN HEMTs at room temperature," *IEEE Trans. Electron Devices.*, vol. 61, no. 12, pp. 4291-4294, Dec. 2014, doi: 10.1109/TED.2014.2361436.

[3] G. A. Kumar, S. Sarmista, S. R. Rosan, and P. Soumya, "Study of temperature variation on threshold voltage and sub-threshold slope of E δ DC MOS transistor including quantum corrections and reduction techniques," *Microsyst. Technol.*, vol. 23, no. 9, pp. 4221-4229, Sep. 2017, doi: 10.1007/s00542-016-2995-z.

[4] S. A. Bota, J. L. Rossello, C. de Benito, A. Keshavarzi, and J. Segura, "Impact of thermal gradients on clock skew and testing," *IEEE Des. Test Comput.*, vol. 23, no. 5, pp. 414-424, Sep. 2006, doi: 10.1109/MDT.2006.126.

[5] P. T. Wang, R. Dawas, M Alwazzan, W. Chang, J. Khan, and C. Li, "Sweating-boosted air cooling using nanoscale CuO wick structures," *Int. J. Heat Mass Transf.*, vol. 111, pp. 817-826, Apr. 2017, doi: 10.1016/j.ijheatmasstransfer.2017.04.042.

[6] R. Singh, A. Akbarzadeh, C. Dixon, M. Mochizuki, and R. R. Riehl, "Miniature Loop Heat Pipe with Flat Evaporator for Cooling Computer CPU," *IEEE Trans. Compon. Packag. Technol.*, vol. 30, no. 1, pp. 42-49, Mar. 2007, doi: 10.1109/TCAPT.2007.892066.

[7] Z. G. Shen, Y. Bai, C. Wang, and J. T. Bai, "Ld end-pumped solid-state cw green laser with air and water hybrid cooling system," *Journal of Applied Optics*, vol. 30, no. 4, pp. 707-711, Apr. 2009, doi: 10.1109/MILCOM.2009.5379889.

[8] J. Garcia, R. D. A. Lara, M. Mohn, H. Schlörb, N. P. Rodriguez, L. Akinsinde, K. Nielsch, G. Schierning, and H. Reith, "Fabrication and modeling of integrated micro-thermoelectric cooler by template-assisted electrochemical deposition," *ECS J. Solid State Sci. Technol.*, vol. 6, pp. N3022-N3028, Jan. 2017, doi: 10.1149/2.0051703jss.

[9] A. Gross, G. Hwang, B. Huang, H. Yang, N. Ghafouri, H. Kim, C. Uher, M. Kaviany, and K. Najafi, "High-performance micro scale thermoelectric cooler: An optimized 6-stage cooler," in *TRANSDUCERS - Int. Conf. Solid-State Sensors, Actuators Microsystems*, 2009, pp. 2413-2416, doi: 10.1109/SENSOR.2009.5285431.

[10] Y. Q. Gan, W. Ge, W. D. Qiao, D. Lu, and J. Lv, "Design and application of TEC controller Using in CCD camera," in *Proc SPIE Int Soc Opt Eng.*, vol. 8196, May. 2011, doi: 10.1117/12.900697.

[11] R. Ahiska and K. Ahiska, "Flexible two phase thermoelectric CPU cooler," *J. Fac. Eng. Archit. Gazi Uni.*, vol. 22, pp. 347-351, Jun. 2007.

[12] B. Abramzon, "Numerical optimization of the thermoelectric cooling devices," *J. Electron Packag. Trans. ASME.*, vol. 129, no. 3, pp. 339-347, Sep. 2007, doi: 10.1115/1.2753959.

[13] Y. Cai, D. Liu, F. Y. Zhao, and J. F. Tang, "Performance analysis and assessment of thermoelectric micro cooler for electronic devices," *Energy Convers. Manage.*, vol. 124, pp. 203-211, Sep. 2016, doi: 10.1016/j.enconman.2016.07.011.

[14] Y. Z. Pan, B. H. Lin, and J. C. Chen, "Performance analysis and

parametric optimal design of an irreversible multi-couple thermoelectric refrigerator under various operating conditions," *Applied Energy*., vol. 84, no. 9, pp. 882-892, Sep. 2007, doi: 10.1016/j.apenergy.2007.02.008.

[15] P. A. J. Stecanella, M. A. A. Faria, and E. G. Domingues, "Eletricity generation using thermoelectric generator – TEG," in *IEEE Int. Conf. Environ. Electr. Eng. EEEIC - Conf. Proc.*, 2015, pp. 2104-2108, doi: 10.1109/EEEIC.2015.7165502.

[16] Z. H. A. Rahman, M. H. M Khir, and Z. A. Burhanudin, "Modeling and simulation analysis of micro thermoelectric generator," in *Int. Conf. Intell. Adv. Syst. ICIAS.*, 2017, pp. 1-5, doi: 10.1109/ICIAS.2016.7824110.

[17] E. F. Sawires, M. I. Eladawy, Y. I. Ismail, and H. A. El-Hamid, "Thermal Resistance Model for Standard CMOS Thermoelectric Generator," *IEEE Access.*, vol. 6, pp. 8123-8132, Jul, 2018, doi: 10.1109/ACCESS.2018.2795382.

[18] K.-I. Hwu, Y.-T. Yau, and M.-L. Hsieh, "Thermoelectric energy conversion system with multiple inputs," *IEEE Trans. Power Electron.*, vol. 35, no. 2, pp. 1603-1621, Feb. 2020, doi: 10.1109/TPEL.2019.2924037.

[19] J. Jeong, M. Shim, J. Maeng, I. Park, and C. Kim, "A high-efficiency charger with adaptive input ripple MPPT for low-power thermoelectric energy harvesting achieving 21% efficiency improvement," *IEEE Trans. Power Electron.*, vol. 35, no. 1, pp. 347-358, Jan. 2020, doi: 10.1109/TPEL.2019.2912030.

[20] J.-M. Amanor-Boadu, A. Mohamed A., and E. Sanchez-Sinencio, "An efficient and fast Li-ion battery charging system using energy harvesting or conventional sources," *IEEE Trans. Power Electron.*, vol. 65, no. 9, pp. 7383-7394, Sep. 2018, doi: 10.1109/TIE.2018.2793243.

[21] T. Martinez, G. Pillonnet, and F. Costa, "A 15-mV inductor-less start-up converter using a piezoelectric transformer for energy harvesting applications," *IEEE Trans. Power Electron.*, vol. 33, no. 3, pp. 2241-2253, Mar. 2018, doi: 10.1109/TPEL.2017.2690804.

[22] N. M. Khattab, and E. T. El Shenawy, "Optimal operation of thermoelectric cooler driven by solar thermoelectric generator," *Energy Conversion and Management*, vol. 47, no. 4, pp. 407-426, Mar. 2006, doi: 10.1016/j.enconman.2005.04.011.

[23] H. Zhang, W. Kong, F. Dong, H. Xu, B. Chen, and M. Ni, "Application of cascading thermoelectric generator and cooler for waste heat recovery from solid oxide fuel cells," *Energy Conversion and Management*, vol. 148, pp. 1382-1390, Sep. 2017, doi: 10.1016/j.enconman.2017.06.089.

[24] L. Lin, Y.-F. Zhang, H.-B. Liu, J.-H. Meng, W.-H. Chen, and X.-D. Wang, "A new configuration design of thermoelectric cooler driven by thermoelectric generator," *Applied Thermal Engineering*, vol. 160, pp. 114087, Sep. 2019, doi: 10.1016/j.applthermaleng.2019.114087.

[25] S. Manikandan, and S. C. Kaushik, "Thermodynamic studies and maximum power point tracking in thermoelectric generator–thermoelectric cooler combined system," *Cryogenics*, vol. 67, pp. 52-62, Apr. 2015, doi: 10.1016/j.cryogenics.2015.01.008.

[26] N. Wang, C. Gao, C. Ding, H. Jia, G. Sui, and X. Gao, "A Thermal Management System to Reuse Thermal Waste Released by High-Power Light-Emitting Diodes," *IEEE Trans. Electron Devices*, vol. 66, no. 11, pp. 4790-4797, Nov. 2019, doi: 10.1109/TED.2019.2938712.

[27] J.-H. Meng, H.-C. Wu, L. Wang, G. Lu, K. Zhang, and W.-M. Yan, "Thermal management of a flexible controlled thermoelectric energy conversion-utilization system using a multi-objective optimization," *Appl. Therm. Eng.*, vol. 179, Oct. 2020, doi: 10.1016/j.applthermaleng.2020.115721.

[28] S. Wiriyasart, and P. Naphon, "Thermal to electrical closed-loop thermoelectric generator with compact heat sink modules," *Int. J. Heat Mass Transf.* vol. 164, Jan. 2021, doi: 10.1016/j.ijheatmasstransfer.2020.120562.

[29] S. Manikandan, S. C. Kaushik, and K. Anusuya, "Thermodynamic modelling and analysis of thermoelectric cooling system," in *Int. Conf. Energy Effic. Technol. Sustain. ICEETS.*, 2016, pp.685-693, doi: 10.1109/ICEETS.2016.7583838.

[30] D. Mitrani, S. Jordi, A. Turó, M. J. García, and J. A. Chávez, "One-dimensional modeling of TE devices considering temperature-dependent parameters using SPICE," *Microelectron. J.*, vol. 40, no. 9, pp. 1398-1405, Sep. 2009, doi: 10.1016/j.mejo.2008.04.001.

[31] A. Mirocha and P. Dziurdzia, "Improved electrothermal model of the thermoelectric generator implemented in SPICE," in *ICSES - ICSES Int. Conf. Signals Electron. Syst. Proc.*, 2008, pp.317-320, doi: 10.1109/ICSES.2008.4673424.

[32] S. Lineykin and S. Ben-Yaakov, "Modeling and analysis of thermoelectric modules," *IEEE Trans. Ind. Appl.*, vol. 43, no. 2, pp. 505-512, Apr. 2007, doi: 10.1109/TIA.2006.889813.